International Journal of Fluid Power 14 (2013) No. 2 pp. 39-51

APPLICATION OF FAST FOURIER AND WAVELET TRANSFORMS TOWARDS ACTUATOR LEAKAGE DIAGNOSIS: A COMPARATIVE STUDY

Amin Yazdanpanah Goharrizi[1] and Nariman Sepehri

Fluid Power and Telerobotics Research Laboratory, Department of Mechanical Engineering,
University of Manitoba, Winnipeg, MB, Canada R3T-5N5
[1] Presently Postdoctoral Fellow, Department of Electrical and Computer Engineering, University of Toronto, Toronto, ON, Canada
Nariman@cc.umanitoba.ca

Abstract

Applications of fast Fourier and wavelet transforms to detect internal leakage in hydraulic actuators are experimentally compared. By analyzing the dynamics of the actuator, it is shown that the internal leakage increases the damping characteristic of the system and decreases the Bode magnitude of pressure signal over valve displacement, around the hydraulic natural frequency. This is further confirmed, by decomposing the original pressure signal, using either transform methods, and identifying the frequency component sensitive to internal leakage. The root mean square of the processed pressure signal is used and a comparison of the two transforms is made to assess their ability to detect internal leakage fault using only pressure signal obtained from either open-loop or closed-loop systems. The results indicate that both approaches can detect internal leakage without a need to explicitly include the model of the actuator and/or the leakage. It is further shown that the wavelet transform method is found to be more sensitive to the internal leakage than the approach based on fast Fourier transform.

Keywords: fault detection, hydraulic actuators, internal leakage, fast Fourier transform, wavelet transform

1 Introduction

Hydraulic systems play an important role in a wide variety of industrial applications: robotics (hydraulic manipulators used in mining and underwater exploration), manufacturing (precision machine tools), aerospace (actuation of aircraft control surfaces) and training (flight simulators). Reliability and safety are important issues in most of the above applications. Thus, condition monitoring of fluid power systems is earning more and more consideration to reduce the cost of maintenance and prevent the system from further deteriorating. Faults in fluid power systems and methods for detecting them have been documented by Watton (2007). This paper focuses on the internal (cross-port) leakage in hydraulic actuators. Internal leakage is caused by the wear of the piston seal that closes the gap between the moveable piston and the cylinder wall. As a result, the hydraulic fluid is displaced between the two chambers of the actuator. Internal leakage affects the dynamic performance of the system since all of the flow provided is not available to move the piston against the load. Often, it cannot be detected until the actuator seal is completely damaged and the actuator fails to respond to a control signal. Research on actuator internal leakage fault identification, in spite of its importance, is still limited. Tan and Sepehri (2002) applied the Volterra nonlinear modeling concept for on-line fault diagnosis in hydraulic systems.

By constructing a parametric space, actuator leakage faults were detected. The technique is similar to the work by Le et al. (1998) who employed neural networks and dynamic feature extraction technique to classify leakage type and level. In both studies, systems with various fault types (including internal leakage) were emulated (through simulations or via experiments) and Volterra/neural network models were developed apriori. An and Sepehri (2005) studied the use of extended Kalman filter (EKF) to detect actuator internal leakage fault. They further extended this work to include both friction and loading as unknown external disturbances (An and Sepehri, 2008). Although the requirement of using a model for internal leakage was removed (An and Sepehri; 2005, 2008), the need for knowing the model of hydraulic actuator and its parameters still remained a challenge. In order to overcome the difficulties associat-

This manuscript was received on 01 December 2012 and was accepted after revision for publication on 28 March 2013

ed with modeling nonlinear hydraulic systems, a linearized model with an adaptive threshold (to compensate for the error due to linearization) was used by Shi et al. (2005) to detect internal leakage fault. Motivated by developing a method that relies less on models of the system or fault, Yazdanpanah and Sepehri (2009, 2010a) showed the successful application of wavelet transforms (WT) toward identification of internal leakage for the class of valve-controlled hydraulic actuators. Using a structured input signal to the valve, the pressure signal at one side of the actuator was decomposed into both scaled and shifted versions of a mother wavelet to detect internal leakage. Performance of the method was successfully tested in experiments. The method was further extended to on-line detection, whereby the actuator is under load and position-regulated (Yazdanpanah and Sepehri, 2010b). More recently, Yazdanpanah and Sepehri (2012) studied the application of empirical mode decomposition (EMD) technique for internal leakage detection and compared its performance with WT. They showed that while EMD is more sensitive to leakage level, WT required smaller computational time than the EMD method.

In this paper, we present new results pertaining to the application of another signal-based technique, the fast Fourier transform (FFT), for internal leakage detection in hydraulic actuators. This work is a significant extension of preliminary work reported earlier by the authors (Yazdanpanah and Sepehri, 2010c). The Fourier transform breaks down a signal into constituent sinusoids of different frequencies and amplitudes. Having small computational time and capability to extract the most prevalent frequency components of a signal, makes this method attractive for some applications. Al-Ammar et al. (2008) used FFT for fault detection in transformer impulse test. Lim et al. (2006) used FFT residuals of the vibration signals for the purpose of fault detection in induction motors. FFT and WT approaches were also compared in some fault detection applications. Gao et al. (2003) employed wavelet transform (WT) for on-line hydraulic pump health diagnosis. They showed that WT was more sensitive and robust than the spectrum analysis approach, in detecting faults associated with hydraulic pumps (Gao et al., 2005). Cusido et al. (2008) applied short-time Fourier transform (STFT) and wavelet decomposition, to investigate fault detection in induction machines and concluded that wavelet analysis achieves better results. To the best of the authors' knowledge, there is no published report on comparing FFT and WT approaches for internal leakage detection in valve-controlled hydraulic actuators. Thus, the second goal of this paper is to compare the efficacy of these two approaches within the context of internal leakage fault detection. This comparison is necessary because one can think that the calculation of the amplitude of the frequency band can be made very straightforward and with precision using the FFT approach. Thus, it may not be necessary to use other tools such WT if FFT works well. Identification of small leakages, ease of implementation and sensitivity to fault levels are key features for this comparison. Additionally, it is known that wear of the actuator cylinder and the seals that cause internal leakage, also changes friction properties of the actuator, which subsequently affect the dynamic performance of the system in a manner similar to internal leakage, (Skormin et al., 1994). Mechanical friction can also change during operation in response to changes in the temperature or lubrication. Isolation of internal leakage in the presence of changing friction properties can be challenging. Thus, the third objective of this paper is to study the effect of changes in friction characteristic of the actuators on performance of both proposed WT- and FFT-based internal leakage fault diagnosis techniques.

The rest of this paper is organized as follows. Section 2, describes the experimental system. Modeling of a typical valve-controlled hydraulic actuator with internal leakage is provided in Section 3. The effect of internal leakage on the Bode magnitude of pressure signals around the hydraulic natural frequency is discussed justifying the choice of sub-band informative signals sensitive to the effect of internal leakage for use by fast Fourier and wavelet transforms. Section 4 provides a brief description of FFT and WT signal processing methods followed by Section 5 that describes how both FFT and WT are experimentally compared towards internal leakage detection. The focus is placed on offline detection of internal leakage where a structured (stationary) input signal is directly applied to the controlled valve. This is another reason one might think using FFT can be good enough for this application. The effectiveness of fast Fourier and wavelet transforms towards on-line internal leakage detection is also examined by applying a pseudorandom reference position input to a loaded position-controlled actuator. Conclusions are provided in Section 6.

2 Experimental System

The photograph of the test-rig, on which all the experiments were carried out, is shown in Fig. 1. The actuator is a double rod type having a 610 mm (24 in) stroke, 38.1 mm (1.5 in) bore diameter, and 25.4 mm (1 in) rod diameter. It is controlled by a high performance Moog D765 servovalve. The actuator is powered by a pump operating at a nominal pressure of 17.2 MPa (2500 psi). The position of the actuator is measured using a cable-driven optical rotary encoder and is monitored by a PC via a Keithley M5312 quadrature incremental encoder card. The PC is also equipped with a DAS-16F input/output board that is used to send the input signal generated by the software to the valve. The DAS-16F is also used to monitor the outputs of all other instruments, which includes a number of pressure transducers and several flowmeters. As illustrated in Fig. 1, the piston seal leakage is emulated by opening a ball valve that connects the two chambers of the actuator. This allows hydraulic fluid to be bypassed across the piston. The level of leakage is controlled by adjusting a needle valve.

The amount of internal leakage flow rate is measured by a positive displacement flowmeter (JVA-KL series by AW Company) with a 7.6 L/min range and an accuracy of 0.5 %. The flowmeter, however, cannot measure the direction of flow. In order to emulate increased actuator friction, two slave cylinders are coupled to the main actuator as shown in Fig. 1.

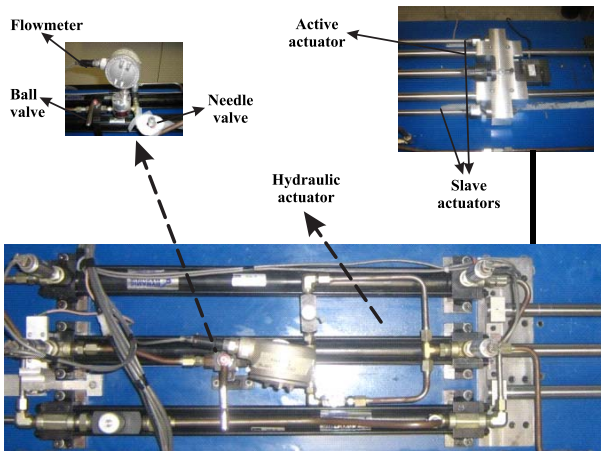

Fig. 1: *Experimental Test-Rig*

3 Modeling and Analysis

Schematic of a valve-controlled hydraulic actuator is shown in Fig. 2.

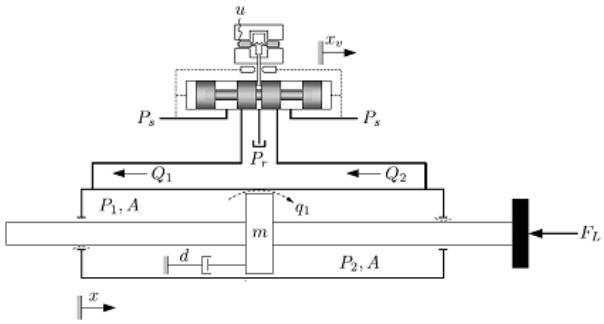

Fig. 2: *Schematic of valve-controlled hydraulic actuator*

The equations that describe the dynamics between control valve input u and the piston position x_p can be formed as (Merritt, 1967):

$$\begin{aligned}
\dot{x}_p &= v_p \\
\dot{v}_p &= \frac{1}{m}(AP_1 - AP_2 - dv_p) \\
\dot{P}_1 &= \frac{\beta}{V + Ax_p}(q_1 - q_l - Av_p) \\
\dot{P}_2 &= \frac{\beta}{V - Ax_p}(-q_2 + q_l + Av_p) \\
\dot{x}_v &= v_v \\
\dot{v}_v &= -w_v^2 x_v - 2\xi w_v v_v + k_v w_v^2 u
\end{aligned} \tag{1}$$

Referring to Eq. 1, the system states are actuator position x_p, actuator velocity v_p, line pressures P_1 and P_2 and valve spool displacement and velocity (x_v,v_v). Parameters m and d are the mass of the load and the effective viscous damping of the actuator, respectively. Parameter A refers to the annulus area of the piston, β is the effective bulk modulus of the hydraulic fluid, V is the volume of fluid contained on either side of the actuator when it is centered. The valve spool dynamics are expressed as a second-order lag where k_v is the valve spool position gain and, parameters w_v and ξ represent the servovalve natural frequency and damping ratio, respectively. For a valve with a critically-lapped spool and having matched and symmetrical orifices, flows q_1 and q_2 through the valve follow the turbulent orifice equation. The nonlinear governing equations can be written in the following forms:

$$\begin{aligned}
q_l &= K_v w x_v \sqrt{\frac{P_s}{2} + \mathrm{sgn}(x_v)(\frac{P_s}{2} - P_1)} \\
q_2 &= K_v w x_v \sqrt{\frac{P_s}{2} + \mathrm{sgn}(x_v)(P_2 - \frac{P_s}{2})}
\end{aligned} \tag{2}$$

In (2) $K_v = C_v\sqrt{\frac{2}{\rho}}$, where C_v is the valve orifice coefficient of discharge, ρ is the density of hydraulic fluid and sgn(*) is the sign function and sgn(0) = 0. Parameter w is the area gradient, and supply pressure is denoted by P_s.

Leakage is a kind of non-ideality that cannot be modeled exactly (Garimella and Yao, 2005). Here, the actuator internal leakage is assumed to be turbulent, and thus follows the following relationship:

$$q_l = K_i\sqrt{|P_1 - P_2|}\,\mathrm{sgn}(P_1 - P_2) \tag{3}$$

K_i is the leakage coefficient whose value depends on the level of leakage fault. Note that q_l is zero for an actuator under normal operating condition. However, when the piston seals begin to wear, leakage of hydraulic fluid across the sealing surfaces occurs. Table 1 shows the values of the parameters used in the nonlinear model, which matches the ones in the experimental test rig (An and Sepehri, 2005; 2008).

Table 1: Parameters of hydraulic actuator

Parameter	Symbol	Value
Supply pressure	P_s	17.2 MPa
Combined mass of piston and rod	m	12.3 Kg
Viscous damping coefficient	d	250 Ns/m
Actuator stroke	L	0.6 m
Piston area	A	633 mm^2
Volume of fluid in either side of actuator	V	234 cm^3
Valve orifice area gradient	w	20.75 mm^2/mm
Valve spool position gain	k_v	0.0406 mm/V
Valve flow coefficient	K_v	0.0292 $m^{3/2}/kg^{1/2}$
Valve natural frequency	w_v	150 Hz
Valve damping ratio	ξ	0.7
Fluid bulk modulus	β	689 MPa

Referring to (1), the first four equations collectively describe the nonlinear dynamics of the actuator, while the last two ones describe the valve spool dynamics. By linearizing the nonlinear dynamics of the actuator about an operating point, *o*, the linearized equations are obtained:

$$\begin{aligned}
\Delta\dot{x}_p &= \Delta v_p \\
\Delta\dot{v}_p &= \frac{1}{m}(A\Delta P_1 - A\Delta P_2 - d\Delta v_p) \\
\Delta\dot{P}_1 &= \frac{\beta}{V}[K_{1f}\Delta x_v - K_{1p}\Delta P_1 - \\
&\quad \frac{K_i}{2\sqrt{|P_{10}-P_{20}|}}\Delta(P_1-P_2) - A\Delta v_p] \\
\Delta\dot{P}_2 &= \frac{\beta}{V}[-K_{2f}\Delta x_v - K_{2p}\Delta P_2 + \\
&\quad \frac{K_i}{2\sqrt{|P_{10}-P_{20}|}}\Delta(P_1-P_2) + A\Delta v_p]
\end{aligned} \tag{4}$$

In (4), Δ denotes a perturbation from the operating, e.g., $\Delta x_p = x_p - x_{p0}$. K_{1f} and K_{2f} are flow gains:

$$\begin{aligned}
K_{1f} &= K_v w\sqrt{\frac{P_s}{2} + \mathrm{sgn}(x_{v0})(\frac{P_s}{2} - P_{10})} \\
K_{2f} &= K_v w\sqrt{\frac{P_s}{2} + \mathrm{sgn}(x_{v0})(P_{20} - \frac{P_s}{2})}
\end{aligned} \tag{5}$$

K_{1p} and K_{2p} are called flow-pressure coefficients:

$$\begin{aligned}
K_{1p} &= \frac{K_v w|x_{v0}|}{2\sqrt{\frac{P_s}{2} + \mathrm{sgn}(x_{v0})(\frac{P_s}{2} - P_{10})}} \\
K_{2p} &= \frac{K_v w|x_{v0}|}{2\sqrt{\frac{P_s}{2} + \mathrm{sgn}(x_{v0})(P_{20} - \frac{P_s}{2})}}
\end{aligned} \tag{6}$$

Note that in deriving the above linearized model, we used the assumption that the variation in the displacement is quite small (Merritt, 1967), i.e., $V >> A|x_p|$

This assumption was necessary to make the theoretical analysis manageable. Furthermore, for an equal area actuator driven by a matched and symmetrical valve, the pressure in one cylinder half rises above $P_s/2$ while the pressure in other cylinder half decreases below $P_s/2$ by roughly the same amount. Thus, for an extending stroke, the individual cylinder pressures are $P_1 \approx 1/2(P_s + P_L)$ and $P_2 \approx 1/2(P_s - P_L)$ where, $P_L = P_1 - P_2$ is the load pressure. Due to the relationship between P_1 and P_2, it is quite often the case that $K_{1f} \approx K_{2f} = K_f$ and $K_{1p} \approx K_{2p} = K_p$ (Merritt, 1967; Karpenko, 2008). The transfer functions relating pressures ΔP_1 and ΔP_2 to spool valve displacement, Δx_v, can now be found as:

$$\frac{\Delta P_1(s)}{\Delta X_v(s)} = \frac{0.5K_f(ms+d)\omega_h^2/A^2}{s^2 + 2\zeta_h\omega_h s + \omega_h^2} \tag{7}$$

$$\frac{\Delta P_2(s)}{\Delta X_v(s)} = \frac{-0.5K_f(ms+d)\omega_h^2/A^2}{s^2 + 2\zeta_h\omega_h s + \omega_h^2} \tag{8}$$

In (7) and (8), $\omega_h = \sqrt{\frac{2\beta A^2}{mV}}$ is the hydraulic natural frequency, $\zeta_h = \frac{dV\omega_h}{4\beta A^2} + \frac{m(K_l + 0.5K_p)\omega_h}{2A^2}$ is the hydraulic damping and $K_l = \frac{K_i}{\sqrt{|P_{10}-P_{20}|}}$.

By studying the transfer functions (7) and (8), it is seen that the internal leakage adds damping to the dynamics of the actuator and this effect intensifies as the leakage level increases. Given the purpose of this paper, it is important to also capture the frequency range within which the pressure signal is sensitive to the internal leakage. The Bode plot of the transfer function (7) is therefore, plotted in Fig. 3, given the parameters in Table. 1. The Bode plot of transfer function (8) displays the results for normal operating condition ($K_i = 0$) as well as for the actuator with internal leakage, ($K_i = 5.83\times10^{-8}\,\mathrm{m^3/\sqrt{Pa}\ s}$). As one can see, internal leakage changes the Bode magnitude around the hydraulic natural frequency, ω_h, which is found to be 70 Hz for the system under investigation. Thus, FFT and WT based techniques that support frequency based behavior and possess analytical strengths to extract specific frequency range, are good choices for the application in this paper.

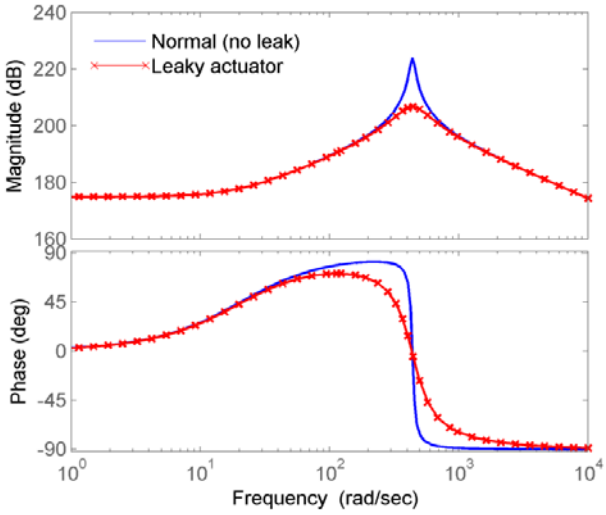

Fig. 3: *Bode plot of transfer function relating pressure to valve displacement for normal and leaky actuator (Yazdanpanah and Sepehri; 2010c)*

4 Methods of Data Processing

4.1 Fourier Analysis

Fourier analysis breaks down a signal into constituent sinusoids of different frequencies. The method can be categorized as continuous Fourier transform (CFT) or discrete Fourier transform (DFT). The Fourier transform of a continuous time signal, $x(t)$, is defined as:

$$X(w) = \int_{-\infty}^{+\infty} e^{-jwt}x(t)dt \tag{9}$$

$X(w)$ is a complex decomposition of the original signal $x(t)$, into constituent exponential functions at each frequency ω and j is the imaginary unit. The discrete Fourier transform, on the other hand, converts a sampled time representation of a signal into a sampled frequency representation. It results in a frequency versus amplitude relationship. The discrete Fourier transform is given as follows:

$$X[n]=\sum_{k=0}^{N-1} x[k]\,e^{-2\pi jnk/N} \qquad n=0,1,...,N-1 \qquad (10)$$

where $x[k]$ is the original signal, N is the length of the original sampled signal vector. DFT can be computed efficiently in practice using a fast Fourier transform algorithm (Proakis and Manolakis, 2007).

4.2 Wavelet Analysis

The wavelet transform (WT) decomposes a signal into levels (also known as scales) with different time and frequency resolutions. As opposed to Fourier analysis that breaks up a signal into sine waves of different frequencies, wavelet analysis breaks up a signal into shifted and scaled version of the original (mother) wavelet. The detailed descriptions of wavelet transform can be found in references by Daubechies (1992) and Vetterli and Herley (1992). Briefly, WT can be continuous or discrete. The continuous wavelet transform (CWT) of a signal $x(t)$ is defined as:

$$\mathrm{CWT}(a,b)=\int_{-\infty}^{+\infty} x(t)\psi_{a,b}(t)dt \qquad (11)$$

where

$$\psi_{a,b}(t)=|a|^{-1/2}\,\psi\left(\frac{t-b}{a}\right) \qquad (12)$$

The mother wavelet $\psi(t) \in L_2(\mathbf{R})$ can be a complex-valued function. The parameters $(a,b \in \mathbf{R})$ are the 'scaling' and 'shifting' parameters, respectively. $|a|^{-1/2}$ is the normalized value of $\psi_{a,b}(t)$ to ensure the length of $\psi_{a,b}(t)$ is the same as $\psi(t)$. For most practical applications, the wavelet coefficients are discretized by a factor of $2^m n$ for shift and by a factor of 2^m for scaling. Equation 11 can then be written as:

$$\mathrm{DWT}(m,n)=2^{-m/2}\int_{-\infty}^{+\infty} x(t)\psi(2^{-m}t-n)dt \qquad (13)$$

where m and n are integers. To implement DWT, the well-known 'multiresolution signal decomposition technique is used. The process starts by applying the low-pass filter (LPF) and high-pass filter (HPF) on the original signal, $x[n]$, decomposing it first into high and low frequency components, $a_1[n]$ and $d_1[n]$, respectively. The decomposition process is continued, with successive approximations being decomposed in turn, so that the original signal is broken down into many lower resolution components.

5 Results and Discussion

As was mentioned earlier, internal leakage introduces damping to the dynamics of the hydraulic actuation system and alters the transient response of the chamber pressures. Here, the sub-band informative signals sensitive to the effect of internal leakage, are obtained by decomposing the original pressure signal at one side of the hydraulic actuator using both fast Fourier transform and wavelet Transform. The effectiveness of both approaches is compared.

5.1 Experiments with Structured Input Signal

First, a periodic (± 1.5 V, 0.5 Hz) square wave signal was applied to the servovalve as the input, which caused the actuator to move back-and-forth (see Fig. 4). This type of input is suitable for off-line applications as it is simple and includes low and high frequency components allowing rich excitation of the pressure signals from which, one can observe the effect of internal leakage. Fig. 4 shows typical pressure responses, given the periodic input signal described above. This input signal is kept the same for all offline tests. The sampling rate at which the data were collected was 500 Hz.

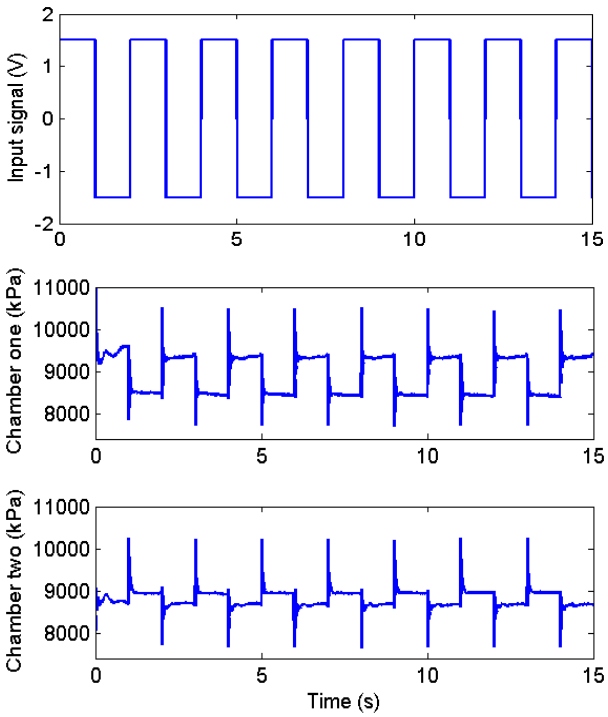

Fig. 4: *Pressure signals in chambers one and two, given a periodic square wave input signal and under normal operating condition*

Next, an internal leakage was introduced given the same input signal as before. Plot of typical leakage is shown in Fig. 5. The corresponding pressure signals are plotted in Fig. 6. Note that internal leakage alters the transient responses in the line pressures, which can be detected by carefully comparing the pressure signals in Fig. 4 and 6. As the internal leakage value becomes smaller, however, the difference between healthy and faulty original pressure signals is less noticeable. Therefore, the original pressure signals cannot provide suffi-

cient information to easily support the actuator health diagnosis when the size of leakage is small; they must be processed to form more informative sub-band signals.

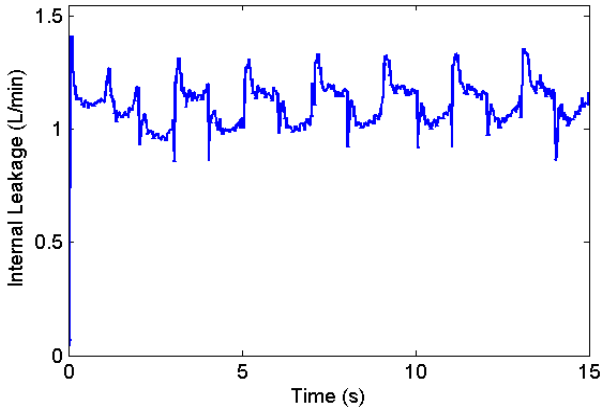

Fig. 5: *Plot of internal leakage flow (mean value of ≈1.1 L/min) for actuator with faulty seal, given a periodic square wave input signal*

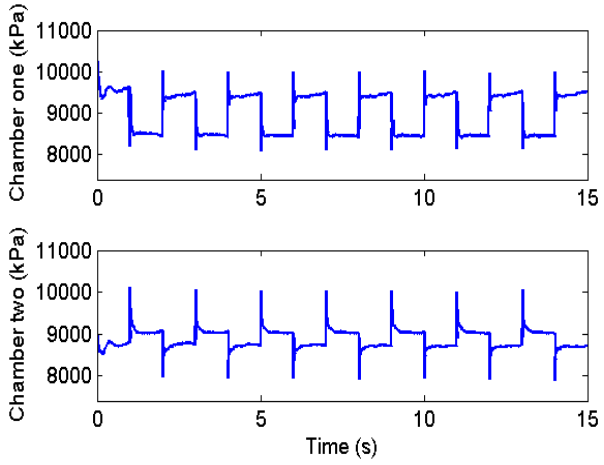

Fig. 6: *Pressures in chambers one and two of hydraulic actuator with internal leakage shown in Fig. 5*

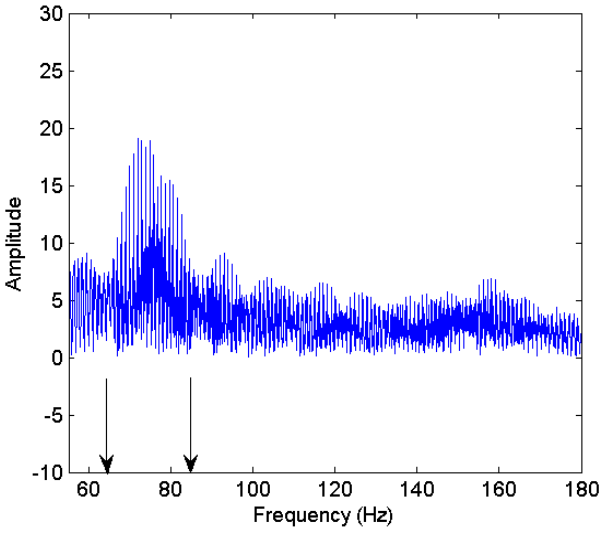

Fig. 7: *Fast Fourier transform of chamber one pressure signal for actuator under normal operating condition*

The results of applying FFT to chamber one pressure signal under normal and faulty (due to internal leakage) operating conditions are shown in Fig. 7 and 8, respectively. From these plots, the feature frequency band is identified to be in the range of 65 to 85 Hz. This is consistent with the frequency band determined by the Bode plot in Section 3.

These results are also in-line with the simulation results obtained using the model represented by the state-space Eq. 1 and documented in Yazdanpanah and Sepehri (2010c). Figures 9 and 10 illustrate the first four detail signals obtained from the pressure in chamber one under normal as well as faulty operating conditions. Daubechies 8 wavelet (Daubechies, 1992) has been used as the mother wavelet. Daubechies wavelets are compactly supported with external phase and highest number of vanishing moments for a given support width (Daubechies, 1992; Ukil and Zivanovic, 2006). Furthermore the associated scaling filters are minimum-phase. Thus, from the view point of implementation, Daubechies wavelet is a good choice for this application (Yazdanpanah and Sepehri, 2010a). Also, a high order mother wavelet is better to avoid overlapping between two adjacent frequency bands (Cusido et al., 2008).

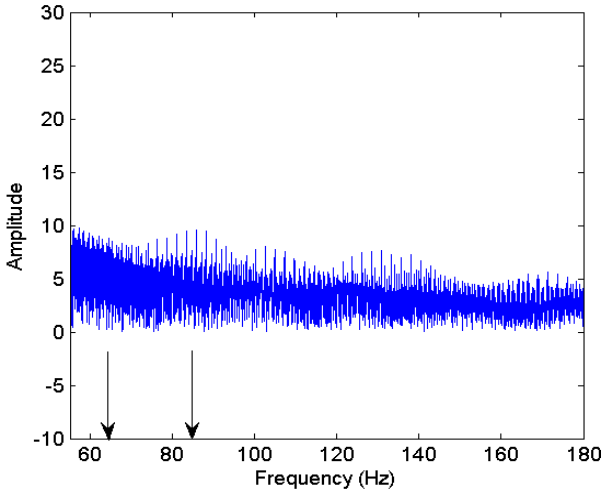

Fig. 8: *FFT of chamber one pressure signal for actuator with internal leakage*

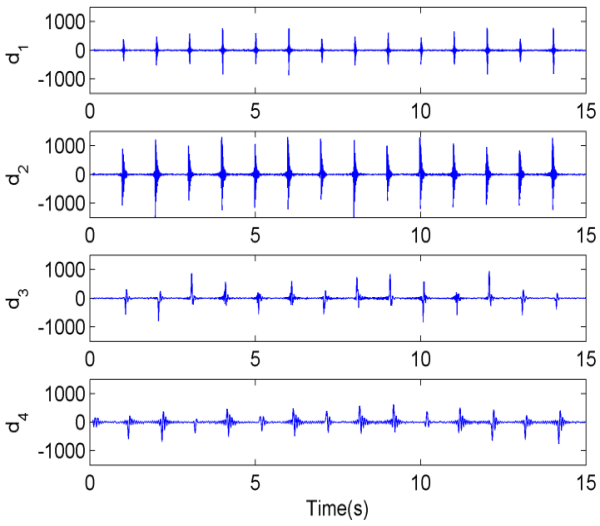

Fig. 9: *First four detail signals of chamber one pressure signal for actuator under normal operating condition*

Note that wavelet transform splits the frequency spectrum into specific frequency bands. The frequency bands depend on the sampling frequency, f_s, as shown in Fig. 11. The highest band, sweeping the frequency from $f_s/2$ to $f_s/4$, belongs to level one decomposition.

For the next decomposition level, this frequency range is divided by two. Referring to Table 2, it is obvious that with four-level of wavelet decomposition, a wide range of frequency can be covered including the frequency range of interest (65 - 85 Hz) represented by coefficient d_2. Furthermore, by comparing Fig. 9 and 10, it is observed that the wavelet coefficient d_2 changes the most, as compared to other coefficients. To facilitate comparison, the root mean square (RMS) values of the processed pressure signal by FFT for frequency band of (65 - 85 HZ), and the wavelet coefficients are calculated. The results are shown in Table 3. From the results, one can observe that the wavelet coefficient, d_2, is more sensitive to the effect of internal leakage than the other wavelet coefficients or the index calculated by the FFT method.

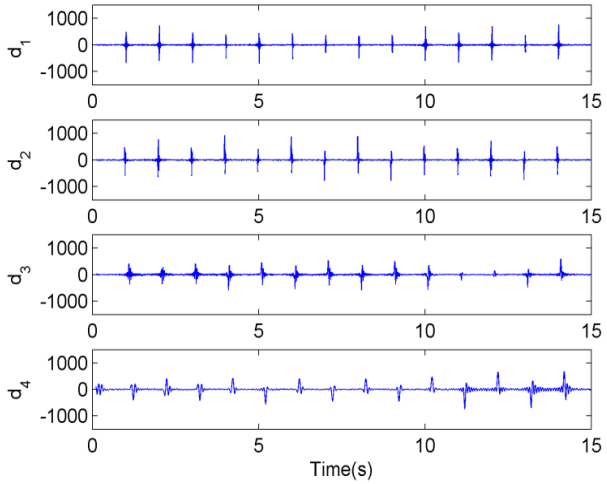

Fig. 10: *First four detail signals of chamber one pressure signal for actuator with internal leakage*

In order to verify the consistency of the results presented so far, the test rig was run 18 times under normal operating condition as well as small and medium leakage situations at various times.

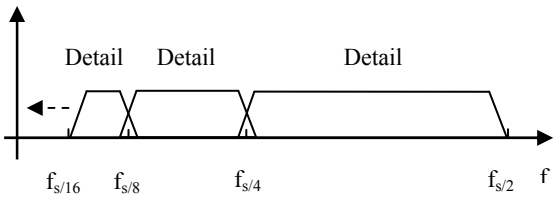

Fig. 11: *Frequency range covered by detail coefficients*

Table 2: Wavelet frequency bands for sampling rate of 500Hz.

Decomposition levels	Frequency bands (Hz)
d_1	250 - 125
d_2	125 - 62.5
d_3	62.5 - 31.25
d_4	31.25 - 15.625

Table 3: RMS values of FFT and four-level wavelet detail coefficients from the measurement of chamber one pressure for normal actuator and actuator with internal leakage shown in Fig. 7.

RMS indices	Healthy Actuator	Faulty Actuator	Percentage of changes
FFT Method (65-85 Hz)	7.01	5.08	27.5
WT Method (d_1)	61	51.2	16
WT Method (d_2)	157.8	79.2	49.8
WT Method (d_3)	93.8	72.4	22.8
WT Method (d_4)	106.8	102.9	3.6

The small leakage (of average 0.124 L/min) that was introduced in this test caused a reduction of ≈ 2.6 % of the available flow rate to the actuator. The medium leakage was of average 0.808 L/min and caused an average reduction of ≈ 17 % of the available flow rate. The average values, reported here, were taken over the entire 18 tests.

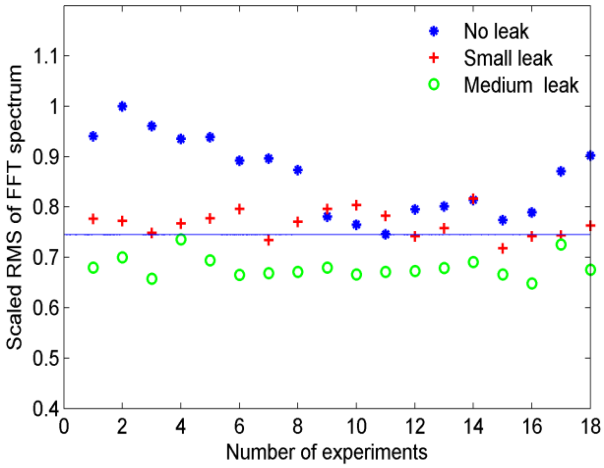

Fig. 12: *Scaled RMS values of FFT spectrum obtained from healthy actuator and actuator experiencing small and medium leakages with mean values of 0.124 and 0.808 L/min. The baseline was chosen as the minimum RMS value obtained from the healthy actuator*

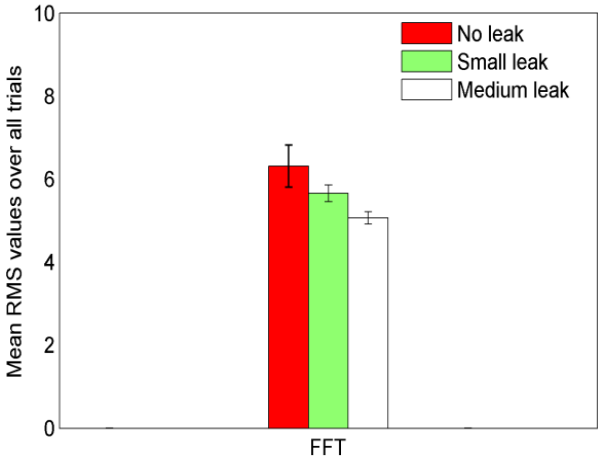

Fig. 13: *Mean RMS and standard deviations taken over all experiments using FFT*

The scaled RMS values using FFT spectrum in the frequency range of interest are shown in Fig 12. Scaling was done by dividing the RMS values by the maximum one to facilitate the comparison. The minimum of RMS values obtained from the FFT under normal operating condition is chosen as a baseline to facilitate comparison. The mean RMS values (from all experiments) as well as standard deviations of the data for normal, small and medium leakages are shown in Fig. 13. The results firstly show that the RMS values of the FFT spectrum of the pressure signal, in the frequency band of interest, reduces with the level of internal leakage. Secondly, the variation of the RMS values over the entire tests is less, as the leakage level increases from no leak to medium leak. The scaled RMS values of detail coefficients, d_1, d_2, d_3 and d_4, obtained from the chamber one pressure signals, at various runs, are shown in Fig. 14 to 17, respectively.

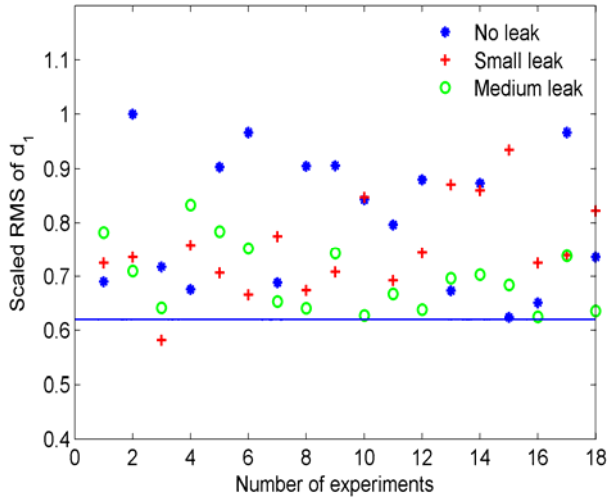

Fig. 14: *Scaled RMS values of detail coefficient, d_1, obtained from healthy actuator and actuator experiencing small and medium leakages with mean values of 0.124 L/min and 0.808 L/min, respectively*

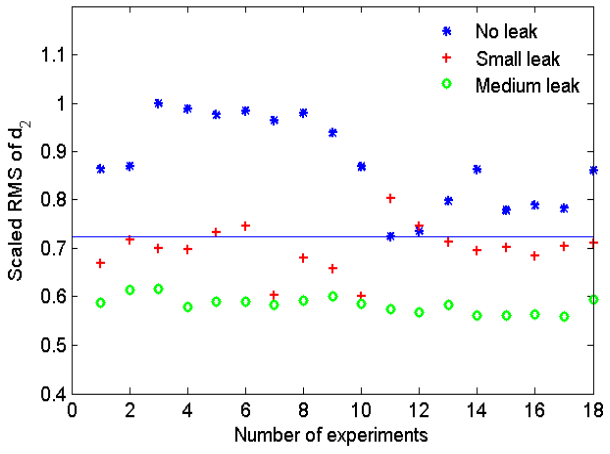

Fig. 15: *Scaled RMS values of detail coefficient, d_2, obtained from healthy actuator and actuator experiencing small and medium leakages with mean values of 0.124 L/min and 0.808 L/min, respectively*

For all these plots baselines were chosen as the minimum RMS value obtained from the healthy actuator. From the results, it is seen that the differences between the RMS values for no leak condition and the RMS values associated with small and medium internal leakages are more noticeable using detail coefficient d_2. The mean values as well as the standard deviations of the data for normal, small and medium leakages are shown in Fig. 18. The results show that the RMS values of the wavelet coefficients obtained from the pressure signal reduce with the level of internal leakage and the variation of the RMS values over the entire tests is less, as the leakage level increases from no leak to medium leak. The change in the standard deviation of the RMS values is believed to be due to the fact that as the internal leakage increases, the effect of damping becomes more dominant masking the effect of dry friction in the form of stick-slip friction that is considered to be somewhat random from experiment to experiment.

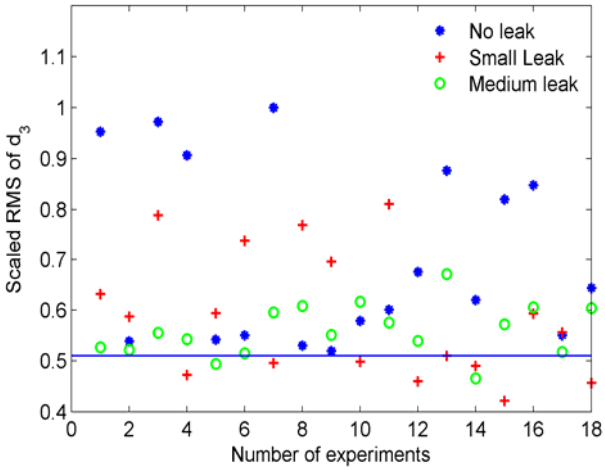

Fig. 16: *Scaled RMS values of detail coefficient, d_3,obtained from healthy actuator and actuator experiencing small and medium leakages*

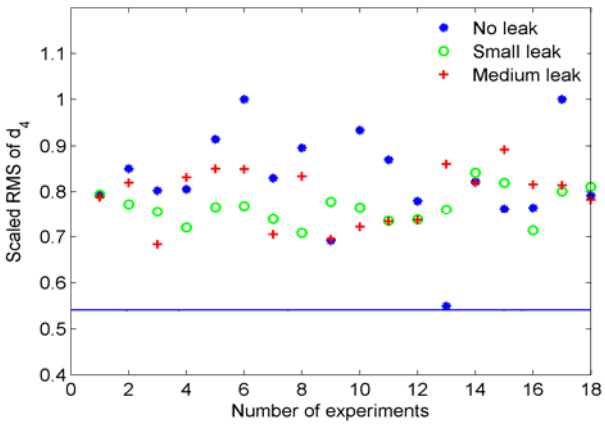

Fig. 17: *Scaled RMS values of detail coefficient, d_4, obtained from healthy actuator and actuator experiencing small and medium leakages*

The percentage of changes of the mean values related to small and medium leakages (over the entire tests) from the mean value of normal operating condition are shown in Fig. 19, using both FFT and WT techniques. It is clearly observed that, as compared to FFT method, the WT technique is more sensitive in detecting internal leakage. For example, with reference to Fig. 12 and 15, small leakage is identifiable 80 % of the times (given the baselines used from the healthy conditions) using WT and only 30 % of the times using FFT.

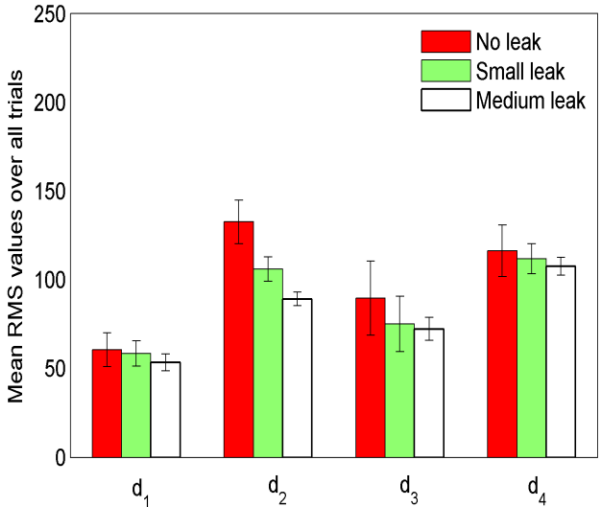

Fig. 18: *Mean RMS and standard deviation taken over all experiments for wavelet coefficients, obtained from healthy actuator and actuator experiencing small and medium leakages*

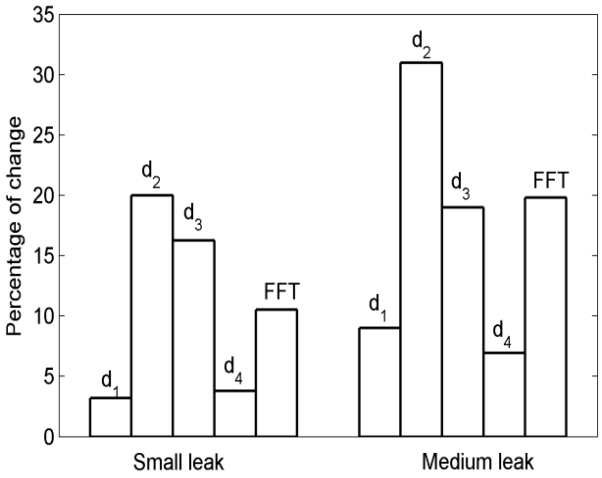

Fig. 19: *Sensitivity of FFT and WT for actuator experiencing small and medium leakages with mean values of 0.124 L/min and 0.808 L/min, respectively*

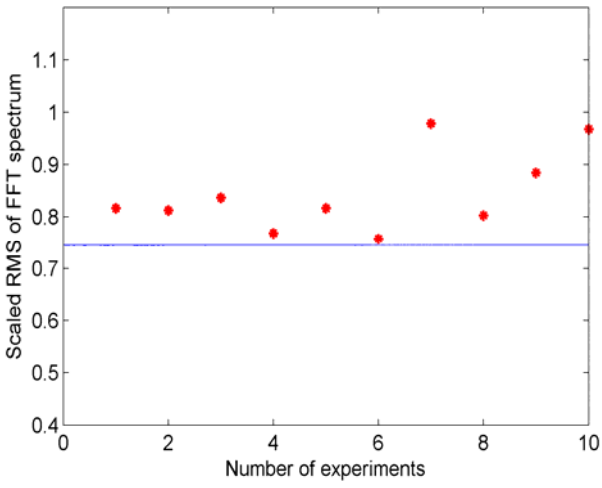

Fig. 20: *RMS values of FFT spectrum obtained from healthy (no leak) actuator with increased friction*

Furthermore, a paired t-test has been conducted for the differences between the baseline value and the RMS values obtained from both FFT and WT methods and, for both small and medium leakage values. A *p* value (probability value) of 0.001 was obtained confirming that WT works better for internal leakage detection than the FFT. Note that a *p* value less than 0.05 indicates that the hypothesis is true (Schervish M. J., 1996).

Remark 1 - As mentioned before, internal leakage is the result of seal wear which also influences the friction property of the actuator. To the best of authors' knowledge, there is no report on the influence of friction changes on internal leakage fault detection techniques prior to this work. Here, we study the effectiveness of both FFT and WT for internal leakage detection of a hydraulic actuator with changing friction properties. By coupling the slave cylinders to the main actuator, the sliding friction of the actuator can be increased from 258 N to 400 N. With reference to Fig. 20 and 21, the test rig was run 10 times under normal (no leak) operating condition using the actuator coupled with slave cylinders (representing increased friction).

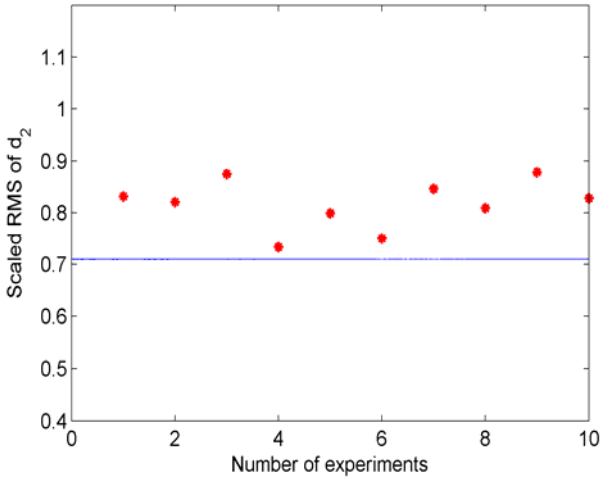

Fig. 21: *RMS values of detail coefficient d_2 obtained from healthy (no leak) actuator with increased friction*

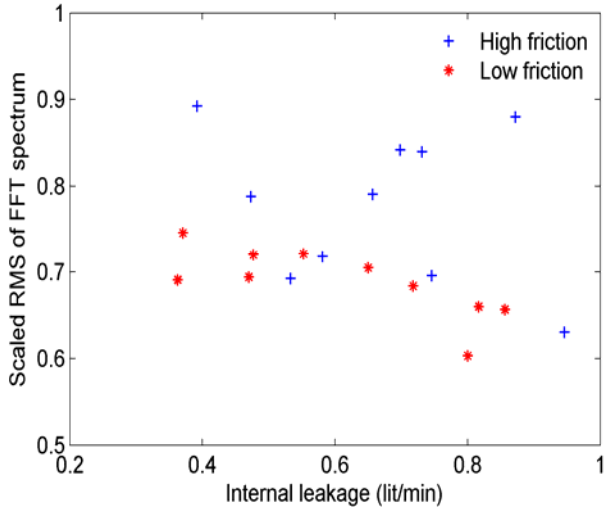

Fig. 22: *RMS values of FFT spectrum obtained from actuator with low and high friction*

As one can see all the RMS values are above the corresponding baselines. Therefore, we can conclude that both methods are not sensitive to the changes in the friction (in the range for which the experiments were performed), which is desirable for the purpose of our

investigation. Next, the effect of increased friction when there is an internal leakage is studied. The trend of RMS values with respect to leakage levels, are illustrated in Fig. 22 and 23 for both FFT and WT schemes.

For this reason, WT is quite sensitive and very effective to capture the internal leakage fault even in the presence of friction. FFT on the other hand, due to its nature of losing the time information of the signal, cannot work as well as WT. This is verified from Fig. 22 and 23.

We can see that, when using WT, the RMS values noticeably decrease with internal leakage for both normal and increased friction. This is due to the fact that internal leakage contributes to changing the transient response of the pressure signal (Le et. al, 1998), while friction can alter both the steady-state as well as the transient responses of pressure signal. The detail coefficient, d_2, having support both in time and in frequency, focuses on the changes in the transient pressure response (abrupt changes) where internal leakage is most influential, and ignores the steady-state effect where friction also contributes.

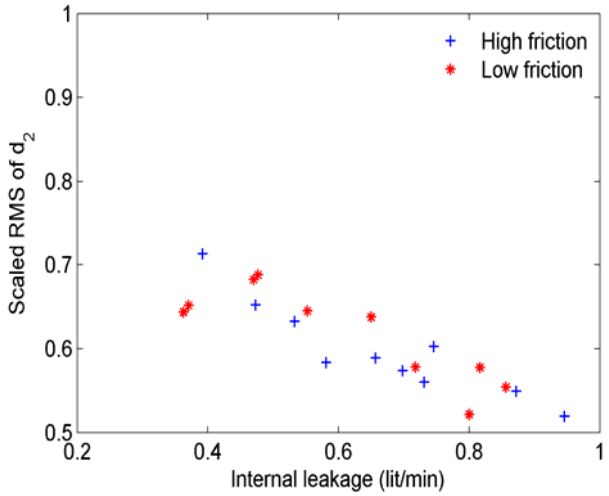

Fig. 23: *RMS values of detail coefficient d_2, obtained from actuator with low and high friction*

Remark 2 - Note that both methods operate on specific frequency area that relates to resonant peak frequency, which can change in real applications as a result of changes in specific parameters of the system. Thus, the issue of robustness of the techniques to the changes of resonant peak frequency becomes important for optimal detection. Two of the parameters that influence the peak frequency and can change with time or temperature are effective bulk modulus and friction. Figure 24(a) shows typical Fourier transform of chamber one pressure signal for the actuator under normal operating condition (similar to Fig. 7). Figure 24(b) shows a similar plot for the same normal actuator, but after many hours of operation to allow the temperature of the hydraulic fluids to rise. From this figure it is seen that, due to changes in some system parameters (as a result of temperature rise) the feature frequency band is shifted. However, its amplitude is not affected. Figure 24(c) shows the Fourier transform of chamber one pressure with the introduction of leakage. As is seen, the amplitude of the feature frequency band is decreased, indicating that as long as the RMS values of the Fourier transform plots are calculated over the proper frequency band, the FFT method works. However, one must shift the interesting range of frequency for optimal diagnosis. Using the WT, on the other hand, the variation of frequency response is still within the range (62.5 - 125 Hz) that can be covered by d_2 (see Table 2). These new results confirm once more that WT is more robust and easier to implement than the FFT.

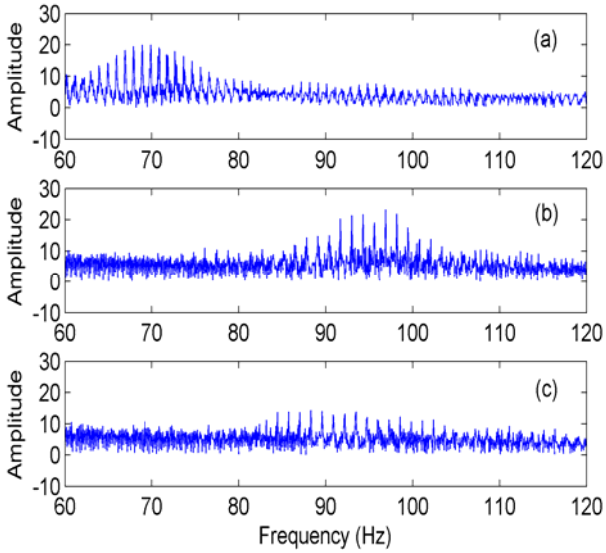

Fig. 24: *Fourier transforms of chamber one pressure signal for the actuator: (a) under normal operating condition (similar to Fig. 7), (b) after many hours of normal operation and (c), under faulty operating condition (leakage of average 0.48 L/min)*

5.2 Experiments with Position Reference Signal

Up to this point, the capability of fast Fourier and Wavelet transforms during offline internal leakage detection has been tested by applying a structured input (periodic steps) directly to the valve under no load condition. Here, the pseudorandom position reference input is employed to examine the effectiveness of these two transforms where the magnitude and duration of the desired actuator position can change. The positioning of the actuator against the spring (as a load) is achieved according to the two-degree-of-freedom feedback system configuration shown in Fig. 25. The controller, $G(s)$, and the prefilter, $F(s)$, are designed to satisfy certain desired closed-loop performance specifications.

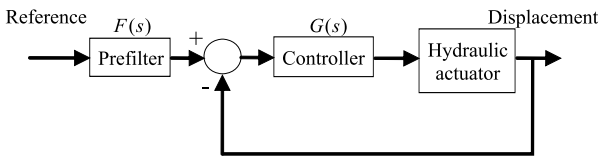

Fig. 25: *Block diagram showing controller and prefilter used for online testing of the methods*

The experiments are conducted with a QFT-based controller with an additional characteristic of holding a desirable performance even in the presence of an internal leakage fault up to 40 % of the rated servovalve flow across the actuator piston. The structure of this controller is shown below:

$$G(s)=\frac{246.59s^3+7.18\times10^3s^2+4.78\times10^7s+5.49\times10^8}{s^3+420s^2+9\times10^4s} \quad (14)$$

$$F(s)=\frac{22.04s+297.5}{s^2+43.5s+297.5} \quad (15)$$

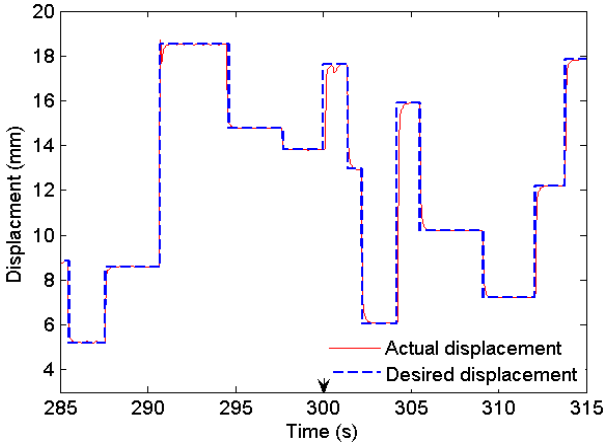

Fig. 26: *Close-up response of actuator with internal leakage introduced after t ≈ 300s. The QFT-based controller is used and the total test time is 600 s*

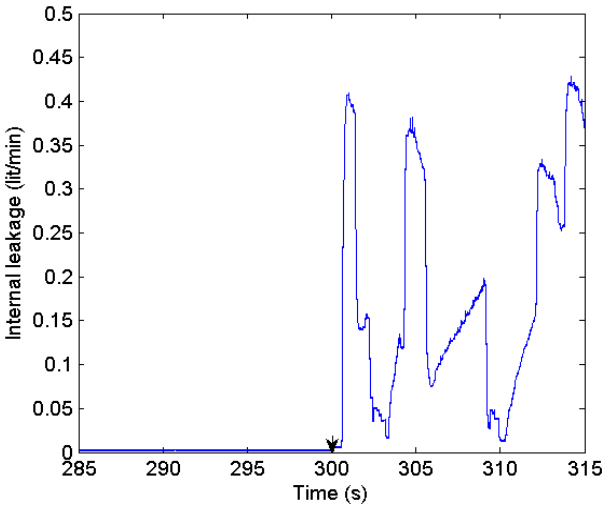

Fig. 27: *Close-up of internal leakage fault (mean value 0.23 L/min)*

The detailed derivation of the QFT controller shown above and its robustness against internal leakage has been reported elsewhere (Karpenko, 2008; Karpenko, and Sepehri, 2010). The pseudorandom signal is characterized with a series of desired step inputs having amplitudes between 0.025 m to 0.05 m and duration between 0.5 s to 4 s. This type of signal resembles activities of flaps for typical in-flight maneuvers. In this experiment a healthy actuator undergoes a set of positioning tasks against a spring having stiffness of 80 kN/m for 600 s. A small internal leakage is then manually introduced at t ≈ 300 s. The close-up plots of displacement and leakage are shown in Fig. 26 and 27, respectively. As one can see the controller works well even after the introduction of internal leakage at t ≈ 300 s, and there is no apparent steady-state error in the position response. This is due to the fact that the controller was designed to be robust to internal leakage. Thus, by only studying the positioning response one cannot locate the occurrence of fault. Fig. 28 shows the FFT of pressure signals during healthy and faulty periods, separately. From Fig. 28, it is seen that the amplitude of the spectrum in the frequency of interest was reduced in the period when the internal leakage was in effect. Fig. 29 shows the plot of wavelet coefficient, d_2, for the entire test period. It is seen that the number, as well as the amplitude of the spikes were noticeably decreased, as a result of internal leakage after t ≈ 300 s.

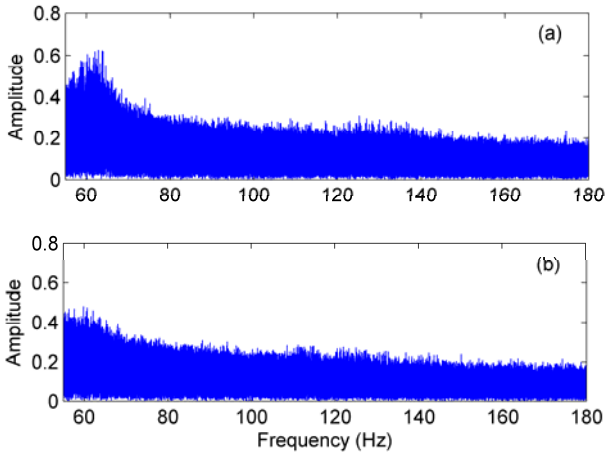

Fig. 28: *FFT spectrum pertaining to experiments shown in Fig. 26 & 27: (a) healthy time period (the first 300 s); (b) faulty time period (the next 300 s)*

Thus, both methods are capable of detecting internal leakage in a loaded closed-loop positioning system. However, FFT cannot reveal the time of occurrence of leakage, whereas, WT locates the time when internal leakage has happened. Thus, WT is more appealing for use in on-line applications.

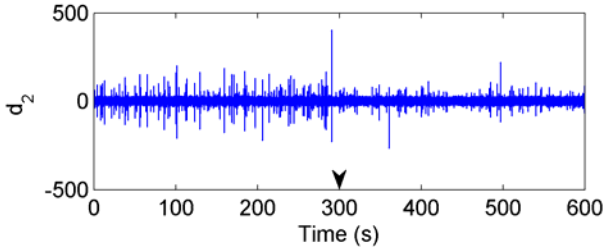

Fig. 29: *Wavelet coefficient d_2 pertaining to experiment shown in Fig. 26 and 27*

6 Conclusions

This paper presented an original application of two well-known techniques, fast Fourier transform (FFT) and wavelet transform (WT) towards internal leakage fault diagnosis. It was shown that the internal leakage decreases the Bode magnitude of pressure signal over the valve spool displacement around the hydraulic natural frequency. Thus, informative sub-band signals, sensitive to the effect of internal leakage, can be extracted from the original pressure signal at either side of the actuator. Fast Fourier transform was employed and the RMS of the FFT spectrum within the feature frequency band was shown to be an appropriate leakage

fault indicator. Similarly, level two detail WT coefficient was shown to be used with confidence for internal leakage diagnosis. Additionally, it was experimentally shown that both FFT and DWT approaches can detect small internal leakages using only one pressure signal and regardless the changes in friction characteristic that can happen simultaneously with internal leakage, in any hydraulic actuator. Thus, both methods can be used with confidence in most practical situations. The results, however, revealed that the WT-based identification is more sensitive in diagnosis of internal leakage than the FFT based approach. This is believed to be due to the fact that wavelets transform having support both in time and in the frequencies, responds better on abrupt behavior in the pressure signal. Thus, the use of WT should be seriously considered when internal leakage fault detection is of concern. Future work should focus on the robustness of the techniques towards optimal detection when other changes in the system can affect the specific frequency area for detection.

Nomenclature

$x(t)$	Signal at time t	
$\psi(t)$	Mother wavelet	
K_{1p}, K_{2p}	Flow-pressure coefficients	[m^3/(Pa s)]
K_{1f}, K_{2f}	Flow gains	[m^2/s]
K_i	Leakage coefficient	[m^3/($\sqrt{Pa}$ s)]
d_i	Detail wavelet coefficient at level i	
P_1, P_2	Pressures in chamber one and two	[kPa]
P_s	Supply pressure	[kPa]
m	Combined mass of piston and rod	[Kg]
d	Viscous damping coefficient	[Ns/m]
L	Actuator stroke	[m]
A	Piston area	[m^2]
V	Volume of fluid	[m^3]
w	Valve orifice area gradient	[m^2/m]
k_v	Valve spool position gain	[m/V]
K_v	Valve flow coefficient	[$m^{3/2}/kg^{1/2}$]
w_v	Valve natural frequency	[Hz]
ξ	Valve damping ratio	
β	Fluid bulk modulus	[MPa]

Acknowledgments

The authors thank the Natural Sciences and Engineering Research Council of Canada (NSERC) who provided financial support for this research.

References

An, L. and **Sepehri, N.** 2005. Hydraulic actuator leakage fault detection using extended Kalman Filter. *Int. Journal of Fluid Power*, Vol. 6, pp. 41 - 51.

An, L. and **Sepehri, N.** 2008. Leakage fault detection in hydraulic actuators subjected to unknown external loading. *Int. Journal of Fluid Power*, Vol. 9, pp. 15 - 25.

Al-Ammar, E., **Karady, G. G.** and **Jin Sim, H.** 2008. Novel technique to improve the fault detection sensitivity in transformer impulse test. *IEEE Trans. on Power Delivery*, Vol. 23, pp. 717 - 725.

Cusido, J., **Romeral, L.**, **Ortega, J. A.**, **Rosero, J. A.** and **Espinosa, A. G.** 2008. Fault detection in induction machines using power spectral density in wavelet decomposition. *IEEE Trans. on Ind. Elec.*, Vol.55, pp. 633 - 643.

Daubechies, I. 1992. Ten lectures on wavelets. Society of Industrial and Applied Mathematics, Philadelphia.

Gao, Y., **Zhang, Q.** and **Kong, X.** 2005. Comparison of hydraulic pump fault diagnosis methods: wavelet vs. spectral analysis. *Proceedings, ASME International Mechanical Engineering Congress and Exposition*, pp. 73 - 78.

Gao, Y. and **Zhang, Q.** 2006. A wavelet packet and residual analysis based method for hydraulic pump health diagnosis. *Proc. IMechE*, 220, pp. 735 - 745.

Garimella, P. and **Yao, B.** 2005. Model based fault detection of an electro-hydraulic cylinder. *American Control Conference*, pp. 484 - 489.

Karpenko, M. 2008. Quantitative fault tolerant control design for a hydraulic actuator with a leaking piston seal. Ph.D. thesis, University of Manitoba.

Karpenko, M. and **Sepehri, N.** 2010. Quantitative fault tolerant control design for a hydraulic actuator with a leaking piston seal. ASME Journal of Dynamic Systems, Measurement, and Control, Vol. 132, No. 5.

Le, T. T., **Watton, J.** and **Pham, D. T.** 1998. Fault classification of fluid power system using a dynamic feature extraction technique and neural networks," *J. of Sys. and Cont. Eng.,* 211, pp. 307 - 317.

Lim, H. S., **Chong, K. T.** and **Su, H.** 2006. Motor fault detection method for vibration signal using FFT residuals. *Int. J. of Applied Elec. and Mech.*, Vol. 24, pp. 209 - 223.

Merritt, H. E. 1967. Hydraulic control systems. John Wiley & Sons, New York.

Mallat, S. 1989. A theory for multiresolution signal decomposition: The wavelet representation. *IEEE Trans. Pattern Analysis and Machine Intelligence*, Vol.11, pp. 674 - 693.

Proakis, J. G. and **Manolakis, D. G.** 2007. *Digital signal processing*, 4th ed. Prentice Hall, 2007.

Shi, Z., **Gu, F.**, **Lennox, B.** and **Ball, A. D.** 2005. The development of an adaptive threshold for model-based fault detection of a nonlinear electro-hydraulic system. *Control Engineering Practice*, Vol. 13, pp. 1357 - 1367.

Skormin, V. A., **Apone, J.** and **Dunphy, J. J.** 1994. On-line diagnostics of a self-contained flight actuator. *IEEE Transactions on Aerospace and Electronic Systems*, Vol. 30, pp. 186 - 195.

Schervish, M. J. 1996. "P Values: What they are and what they are not". *The American Statistician,* Vol. 50, pp. 203 - 206.

Tan, H. and **Sepehri, N.** 2002. Parametric fault diagnosis for electrohydraulic cylinder drive units. *IEEE Trans. Industrial Electronics*, Vol. 49, pp. 96 - 106.

Ukil, A. and **Zivanovic, R.** 2006. Abrupt change detection in power system fault analysis using adaptive whitening filter and wavelet transform. *Elec. power Sys. Research*, Vol.76, pp. 815 - 823.

Vetterli, M. and **Herley, C.** 1992. Wavelets and filter banks: Theory and design. *IEEE Tran. Signal Processing*, Vol. 40, pp. 2207 - 2232.

Watton, J. 2007. Modeling, monitoring and diagnostic techniques for fluid power systems, Springer.

Yazdanpanah-Goharrizi, A. and **Sepehri N.** 2009. Internal leakage diagnosis in hydraulic actuators using wavelet transform. *ASME Dynamic Systems and Control Conference*, California, USA.

Yazdanpanah-Goharrizi A. and **Sepehri N.** (2010a). Off-line internal seal damage diagnosis in hydraulic cylinder drives using wavelet analysis. *IEEE Transaction on Industrial Electronics*, Vol. 57, no. 5, pp. 1755 - 1762.

Yazdanpanah-Goharrizi, A. and **Sepehri N.** (2010b). A wavelet based approach for diagnosis of internal leakage in hydraulic actuators using on-line measurements. *Int. Journal of Fluid Power*, Vol. 11, no.1, pp. 61 - 69.

Yazdanpanah-Goharrizi, A. and **Sepehri N.** (2010c). Application of Fourier transform for actuator leakage diagnosis. *ASME/Bath Symposium on Fluid Power and Motion Control*, Bath, UK.

Yazdanpanah-Goharrizi, A. and **Sepehri N.** (2012). Internal leakage detection in hydraulic actuators using empirical mode decomposition and Hilbert spectrum. *IEEE Transaction on Instrumentation and Measurement*, Vol. 61, pp. 368 - 378.

Amin Yazdanpanah Goharrizi
received his B.S. degree from Amirkabir University of Technology, Tehran, Iran, in 2003, and his M.Sc. degree from Khajeh Nasir University, Tehran, Iran, in 2005 and his Ph.D. degree from the University of Manitoba, Canada. Currently, he is a jointly appointed Postdoctoral Fellow at the University of Toronto and Sunnybrook Health Sciences Centre. His current research interests include fault detection, signal processing and control systems.

Nariman Sepehri
is a professor with the Department of Mechanical and Manufacturing Engineering, at the University of Manitoba, Canada. His research and development activities are primarily centered in all fluid power related aspects of systems, diagnosis and control.